J. Indian Chem. Soc.,
Vol. 94, April 2017, pp. 409-417

Steady state kinetics of formation of oxide films on niobium and tantalum metals in malic acid electrolyte at different temperatures

Naveen Verma*, Jitender Jindal and Krishan Chander Singh

Department of Chemistry, Maharshi Dayanand University, Rohtak-124 001, Haryana, India

E-mail : vermanaveen17@gmail.com

Manuscript received online 30 November 2016, accepted 10 December 2016

Abstract : Steady state kinetic data from anodic polarization of niobium and tantalum metals under galvanostatic conditions have been obtained over wide range of temperatures and at different current densities in malic acid electrolyte. The obtained data has been analyzed in the light of various theories of ionic conduction. The value of constant *A* in Guntherschulze and Betz equation is temperature dependent while *B* is independent of temperature. The constant *A* is also dependent on the nature of the electrolyte. The data indicates the temperature independent Tafel slope which rules out the applicability of the single barrier theory of Cabrera and Mott. The data has been analyzed in terms of Dignam's equation. The effects of current density and temperature in aqueous electrolyte on various parameters of Dignam's equation have been examined.

Keywords : Tantalum, niobium, malic acid, Tafel slope.

Introduction

Anodization is an electrolytic passivation process which involves the production of oxide film on the metallic substrate[1,2]. It removes electrons from the substrate causes oxidation of anode. In the process of anodic oxidation, the electrode kinetic feature of surface is the critical one. It is extremely complicated to develop anodic oxide film on metal under high field strength because of the vicinity of metal/oxide and oxide/solution interface at which transfer processes must happen.

Galvanostatic[3–5], potentiostatic anodization[6–9] and the sequence of both[4] are the techniques for anodic oxide film growth on metals. The parameters highly influence the oxide film characteristics are the type and concentration of electrolytic solution, electrolytic pH, temperature of electrolyte and the applied current density or voltage[10,11]. Galvanostatic anodization is better than potentiostatic anodization due to the fact that, in later, the current decreases abruptly until the leakage current pre-dominates or recrystallization begins.

In the steady state galvanostatic anodization, the potential increases steadily with time due to the formation of the anodic oxide layer[12]. Because of this behavior, electric field inside the film formed, remains constant. In this way, all anodic current density is used in the film formation in states of high field.

According to the Guntherschulze and Betz model[13], high field ionic conduction equation for kinetics of growth of film on metals is represented by

$$\ln i = \ln A + BE \quad (1)$$

where i = flux density of ionic species i.e. current density, E = electric field strength in the film and A and B are the constants.

Various different models, additionally proposed, to clarify the growth kinetics of the oxide film formation by different researchers. Cabrera and Mott model clarify that the Tafel slope must be proportional to temperature. Young, Vermilyea and others disagreed with Cabrera Mott model; the discovered Tafel slope must be independent of the temperature[14].

Numerous efforts have been proposed to consider the growth kinetics of anodic oxide film formation on different valve metals by investigators[15–17]. In this section, we examine the development of anodic oxide film on niobium and tantalum metals at different current densities and temperatures in aqueous electrolyte such as malic acid. The behavior of Tafel slope and selective consideration of dif-

ferent ionic conduction theories with special reference to Dignam's methodology has been made.

Experimental

Niobium and tantalum samples with 2 cm^2 exposed area, with a short tag were cut by a dye from metal sheet (99.8% pure). The edges and surface of samples were rubbed with 600; 1000; 1500; 2000 grit fine grade emery paper to make the surface smooth. The specimens were dipped into 100 g/L KOH solution at temperature 80 °C for 3 min with constant stirring to remove the greasy particles, and then washed with double distilled water. Chemical polishing of the sample was done by dipping in freshly prepared etching mixture of 98% H_2SO_4; 70% HNO_3; 48% HF (5 : 2 : 2 v/v) for 3–5 s in Teflon beaker and then immediately washed with distilled water. Finally, any remaining polluting influence left adhering to the surface, was evacuated by putting the specimen in boiled water for 10 min. Finally, the sample was dried in a stream of hot air. The whole process was repeated again just before the use of the sample. The above procedure of surface preparation was found to give a steady rate of film growth in the process of anodic oxidation of specimens under constant current density conditions. Working area of specimen sample was defined by making a thick anodic oxide film on tag in 0.1 *N* citric acid solution at room temperature. Some oxide layer was always formed on the square portion of specimen surface due to the creep age of electrolyte during the formation of film on tag. This additional layer formed, was removed by dipping square portion of the sample in 50 g/L KOH at temperature 80 °C up to the required depth. The square portion was washed, chemically polished and placed in boiling water as described earlier. In this way, oxide layer formation not takes place on tag during anodic oxidation of electrode and the working area was exactly 2 cm^2.

The above prepared specimen was immersed in a Pyrex glass cell. Pt wire cross section dipped in this cell act as cathode in the anodic oxidation process. The temperature of this cell was controlled with a steady temperature control regulator (thermostat).

Niobium and tantalum samples were anodically polarized at steady current density, with the help of current source meter (Keithley 2400). The film was formed on the metal specimens up to a desired voltage. The growth kinetics for the anodic oxide film on metal specimens were carried out at different current densities (2.5; 5.0; 10.0 and 15.0 mA/cm^2) in 0.1 *M* malic acid electrolyte at four unique temperatures 20; 30; 40; 50 °C. The thickness of film is controlled by using Faraday's law.

Results and discussion

Figs. 1 and 2 shows the plot between formation voltage and anodization time of Nb and Ta metal respectively, which demonstrates that the rate of growth of oxide film is abruptly increases up to 160 V. During the complete anodization, the colour of oxide film fluctuates ceaselessly and at breakdown voltage the colour goes dark grey and the surface become slightly rough because of some local crystallization of Ta_2O_5.

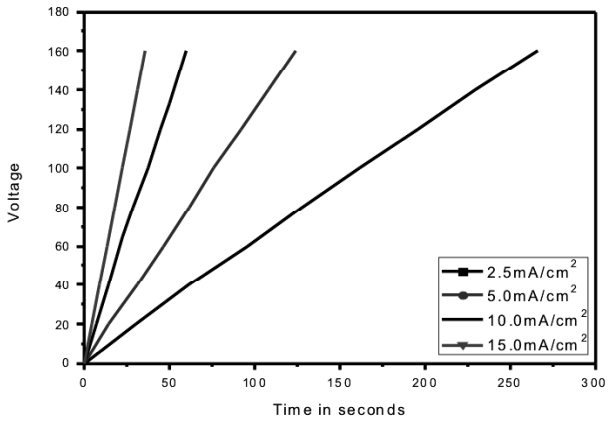

Fig. 1. Variation of voltage of formation with time of anodization of niobium metal in malic acid.

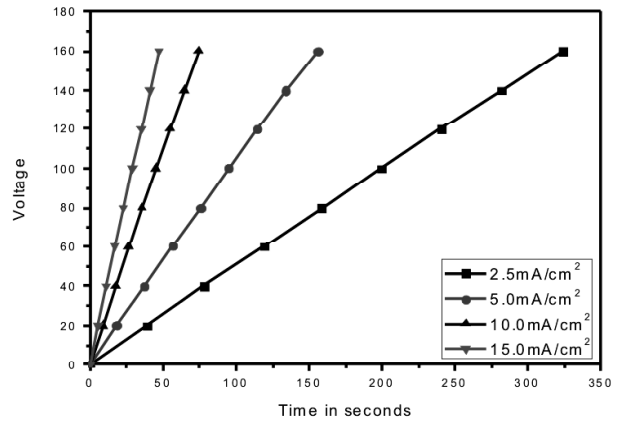

Fig. 2. Variation of voltage of formation with time of anodization of tantalum metal in malic acid.

Thin film interference is responsible for the colour of oxide film which further relies on the oxide film thickness. The resulted oxide film is transparent and has a high refractive index. Light waves bounce off the oxide, however some go through and reflect off the metal beneath, reappearing on the surface after a time gap that depends on the thickness of the oxide layer. Those two sets of the wave either interfere with or strengthen one another, making the colour visible[18]. Figs. 1 and 2 demonstrates the linear relationship between voltage and time up to 160 V, which means that, the field strength inside the film is stable and is almost independent of film thickness. Figs. 3 and 4 demonstrates the plots of field (E) versus reciprocal of temperature at varied current densities are straight and parallel and have slope $\delta E/(\delta 1/T)$. These graphs demonstrate the reciprocal relationship between temperature and field quality at constant current density i.e. with increase of temperature, the value of field strength, E decreases.

Tables 3 and 4 represent the value of field strength for different current densities at various temperatures for niobium and tantalum metals separately. Information of above tables has been broken down by different current hypotheses of ionic conduction.

Tables 5 and 6 represent the value of constant A and B which is calculated by least square method for various temperature ranges by applying Guntherschulze and Betz empirical equation. The validity of this equation was confirmed at different current densities. The value of constant A differs with temperature, yet there is no significant variation in the values of constant B, explaining that the value of B to be independent of temperature. The value of A and B, however vary with nature of aqueous electrolyte.

According to the single barrier theory of Cabrera and Mott for ionic growth, E is given by

$$E = \frac{kT}{bq} \ln \frac{i}{N_s \vartheta_s q} + \frac{\varphi}{bq} \tag{2}$$

where N_s is the number of ions cm^{-2} of the metal surface, ϑ_s is their vibrational frequency normal to the barrier and φ is the potential barrier opposing entry into the oxide as the rate determining step.

As per this hypothesis, the Tafel slope ($\delta E/\delta \ln i$) must be directly proportional to the absolute temperature. Figs. 5 and 6 represents the plot between E versus $\ln i$, gives the constant value of Tafel slope at various temperatures, thus the applicability of this hypothesis was ruled out. The plot of E versus $1/T$ (Figs. 3 and 4) at different current densities is parallel lines demonstrating the possible existence of space charge in the film.

Young[19] observed a field dependent Tafel slope $\delta E/\delta \ln i$ and its dependence was accounted by the equation

$$I = I_0 \exp\left\{\frac{-Q - \alpha E + \gamma E^2}{kT}\right\} \tag{3}$$

where Q, α and γ are all the positive constants and K is Boltzmann constant.

Dignam[20,21] is attempted to clarify the field and tem-

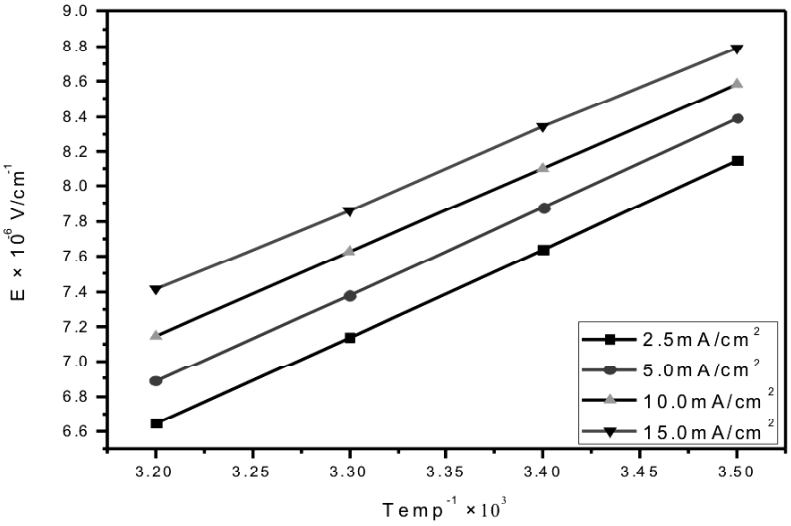

Fig. 3. Plot of E vs T^{-1} (niobium metal).

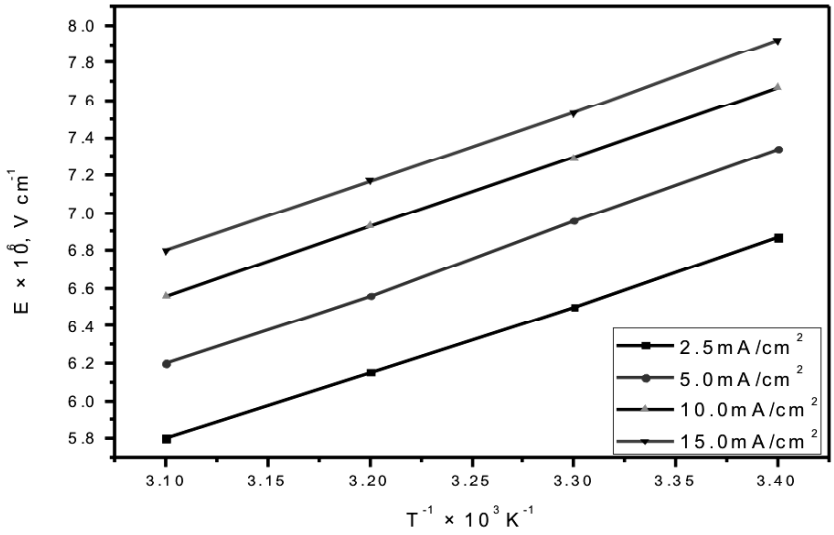

Fig. 4. Plot of E vs T^{-1} (tantaum metal).

Table 1. Anodic oxide film formation on niobium in 0.1 *M* malic acid at various temperatures and at different current densities

Voltage of formation	Charge×10^3 (*C*)	Field×10^{-6} *V* (cm)	Charge×10^3 (*C*)	Field×10^{-6} *V* (cm)	Charge×10^3 (*C*)	Field×10^{-6} *V* (cm)	Charge×10^3 (*C*)	Field×10^{-6} *V* (cm)
	2.5 mA (cm^2)		5.0 mA (cm^2)		10.0 mA (cm^2)		15.0 mA (cm^2)	
	Temperature of study 293.15 K							
20	75	8.46	72	8.81	70	9.07	60	10.58
40	155	8.19	154	8.24	140	9.07	130	9.76
60	238	8.00	230	8.28	225	8.46	200	9.52
80	320	7.93	310	8.19	285	8.91	270	9.40
100	405	7.83	380	8.35	375	8.46	330	9.62
120	490	7.77	460	8.28	450	8.46	400	9.52
140	575	7.72	540	8.23	500	8.88	470	9.45
160	665	7.75	620	8.19	600	8.46	540	9.40
	Temperature of study 303.15 K							
20	77	8.24	74	8.58	70	9.07	70	9.07
40	160	7.93	160	7.93	150	8.46	130	9.76
60	247	7.71	240	7.93	225	8.46	210	9.07
80	337	7.53	320	7.93	300	8.46	280	9.07
100	430	7.38	400	7.93	385	8.24	340	9.33
120	515	7.39	480	7.93	465	8.19	410	9.29
140	600	7.40	560	7.93	525	8.46	480	9.25
160	700	7.25	646	7.86	615	8.25	450	9.23
	Temperature of study 313.15 K							
20	80	7.93	80	7.93	75	8.46	70	9.07
40	172	7.38	164	7.74	150	8.46	140	9.07
60	265	7.18	250	7.61	245	7.77	210	9.07
80	355	7.15	330	7.69	320	7.93	290	8.75
100	440	7.21	420	7.55	400	7.93	360	8.81
120	525	7.25	500	7.61	480	7.93	430	8.85
140	615	7.22	580	7.66	565	7.86	500	8.88
160	705	7.20	660	7.69	640	7.93	580	8.75

Table-1 (contd.)

				Temperature of study 323.15 K				
20	85	7.46	86	7.38	80	7.93	70	9.07
40	175	7.25	170	7.46	165	7.69	140	9.07
60	266	7.16	260	7.32	250	7.61	220	8.65
80	360	7.05	340	7.46	325	7.81	300	8.46
100	445	7.13	430	7.38	410	7.74	380	8.35
120	535	7.12	510	7.46	490	7.77	450	8.46
140	625	7.11	600	7.40	575	7.72	520	8.54
160	720	7.05	680	7.46	650	7.81	600	8.46

Table 2. Formation of oxide film on tantalum in 0.1 *M* malic acid at various temperatures and at different current densities

Voltage of formation	Charge $\times 10^3$ (*C*)	Field $\times 10^{-6}$ *V* (cm)	Charge $\times 10^3$ (*C*)	Field $\times 10^{-6}$ *V* (cm)	Charge $\times 10^3$ (*C*)	Field $\times 10^{-6}$ *V* (cm)	Charge $\times 10^3$ (*C*)	Field $\times 10^{-6}$ *V* (cm)
	2.5 mA (cm^2)		5.0 mA (cm^2)		10.0 mA (cm^2)		15.0 mA (cm^2)	
				Temperature of study 293.15 K				
20	97	7.14	90	7.70	86	8.06	82	8.45
40	195	7.10	184	7.53	174	7.97	166	8.36
60	297	7.00	281	7.40	262	7.93	255	8.14
80	396	6.96	378	7.34	353	7.86	344	8.06
100	498	6.93	474	7.32	448	7.74	433	8.01
120	601	6.92	572	7.28	546	7.62	523	7.96
140	704	6.90	671	7.24	644	7.54	613	7.92
160	809	6.86	780	7.12	744	7.46	708	7.84
				Temperature of study 303.15 K				
20	97	7.14	94	7.37	90	7.70	85	8.16
40	207	6.70	194	7.15	188	7.38	179	7.75
60	314	6.62	298	6.97	286	7.28	273	7.62
80	424	6.54	404	6.86	382	7.26	367	7.56
100	535	6.48	507	6.84	479	7.24	461	7.52
120	643	6.48	616	6.76	578	7.20	557	7.48
140	757	6.42	712	6.74	678	7.16	651	7.46
160	873	6.36	826	6.72	784	7.08	752	7.38
				Temperature of study 313.15 K				
20	103	6.73	96	7.22	90	7.64	87	7.92
40	221	6.28	206	6.74	183	7.18	188	7.36
60	322	6.46	310	6.70	295	7.06	286	7.28
80	449	6.18	415	6.68	400	6.94	387	7.16
100	572	6.07	523	6.63	505	6.87	493	7.04
120	697	5.97	637	6.52	616	6.76	598	6.96
140	821	5.92	757	6.42	719	6.76	710	6.84
160	943	5.86	870	6.38	831	6.68	826	6.72
				Temperature of study 323.15 K				
20	107	6.47	102	6.75	96	7.16	92	7.50
40	227	6.10	219	6.32	206	6.72	193	7.18
60	349	5.96	330	6.30	313	6.64	301	6.92
80	467	5.94	445	6.24	426	6.52	404	6.86
100	592	5.86	561	6.18	537	6.46	509	6.82
120	713	5.84	689	6.04	651	6.40	618	6.74
140	814	5.78	804	6.04	764	6.36	732	6.64
160	983	5.76	932	6.01	884	6.28	852	6.52

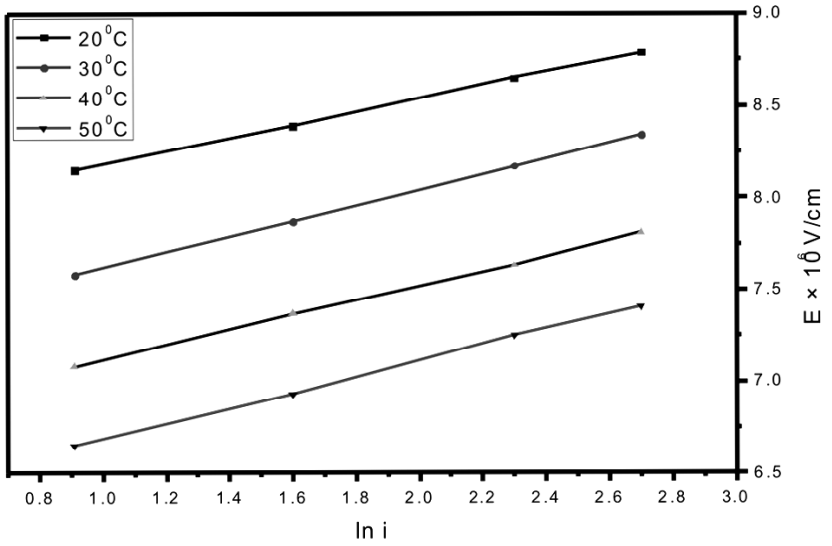

Fig. 5. Plot of E vs ln i (i in A/cm^2) for niobium metal.

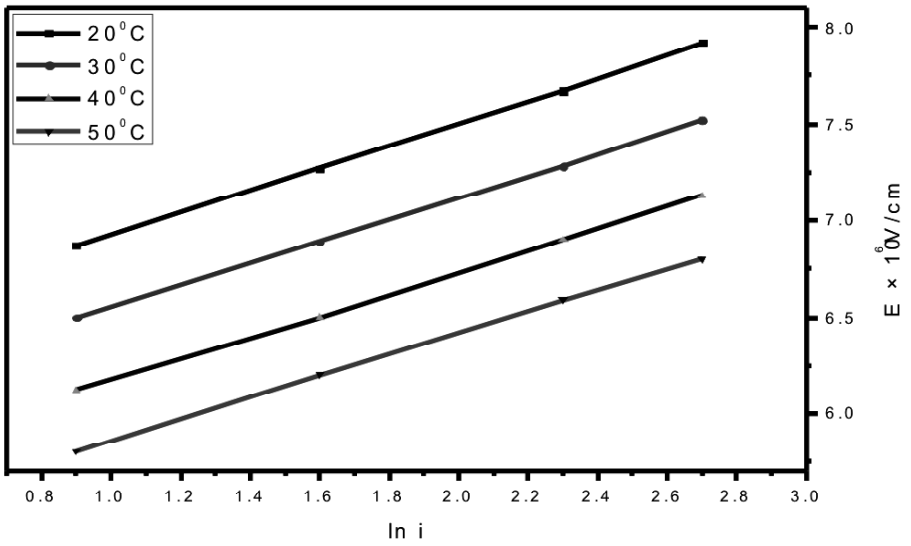

Fig. 6. Plot of E vs ln i (i in A/cm^2) for tantalum metal.

Table 3. Mean fields of niobium at different current densities and temperatures in 0.1 *M* malic acid electrolyte

Current density	Field (E)$\times 10^{-6}$ V (cm)			
mA (cm^2)	293.15 K	303.15 K	313.15 K	323.15 K
2.5	8.15	7.58	7.13	6.65
5.0	8.39	7.82	7.37	6.99
10.0	8.58	8.01	7.63	7.15
15.0	8.79	8.34	7.81	7.41

Table 4. Mean fields of tantalum at different current densities and temperatures in 0.1 *M* malic acid electrolyte

Current density	Field (E)$\times 10^{-6}$ V (cm)			
mA (cm^2)	293.15 K	303.15 K	313.15 K	323.15 K
2.5	6.87	6.50	6.12	5.80
5.0	7.34	6.92	6.56	6.20
10.0	7.67	7.25	6.90	6.56
15.0	7.92	7.52	7.13	6.80

perature dependence of Tafel slope for steady state anodic oxidation of Nb, Ta and other valve metals by considering a straightforward model, as indicated by which the field independent component of potential energy function

Table 5. Values of parameters *A* and *B* of Guntherschulz and Betz equation for various aqueous electrolytes at different temperatures of niobium metal

Temperature (K)	*A* (A/cm)	*B* (cm/V)
	Electrolyte : 0.1 *M* malic acid	
293.15	0.60×10^{-16}	3.72×10^{-6}
303.15	3.17×10^{-14}	3.19×10^{-6}
313.15	2.70×10^{-14}	3.40×10^{-6}
323.15	3.88×10^{-13}	3.23×10^{-6}

Table 6. Values of parameters *A* and *B* of Guntherschulz and Betz equation for various aqueous electrolytes at different temperatures of tantalum metal

Temperature (K)	*A* (A/cm)	*B* (cm/V)
	Electrolyte : 0.1 *M* malic acid	
293.15	1.0×10^{-8}	1.778×10^{-6}
303.15	2.0×10^{-8}	1.798×10^{-6}
313.15	4.0×10^{-8}	1.798×10^{-6}
323.15	6.9×10^{-8}	1.808×10^{-6}

for displacement of a mobile charged species is expected to resemble a Morse function. According to steady state data for anodic oxidation for these metals were represented inside experimental error by just three exponential constant, the experimental variable, the activation energy and Morse function distance parameter. The ionic conduction equation is given by

$$I = I_0 \exp\left\{-\frac{\left[\varphi-\mu^*\left(1-\frac{\mu^* E}{C\varphi}\right)\right]}{kT}\right\} \tag{4}$$

where I_0 is the primary current density, φ is the zero field activation energy, C is a dimensionless quantity and μ* is the zero field activation dipole. Parameter μ*, φ and C are not independent constant but are related through the form of potential energy function.

From eq. (4), value of E

$$E = C\varphi/2\mu^*\left[1-\frac{4}{C}-\frac{4kT}{C\varphi}\ln\frac{i}{i_0}\left\{\left(\frac{i}{i_0}\right)\right\}^{\frac{1}{2}}\right] \tag{5}$$

Young[18] observed a field dependent Tafel slope $\delta E/\delta \ln i$ and this dependence was accounted by the equation

$$\frac{\delta E}{\delta\left(\frac{1}{T}\right)} = S = -\left(\frac{kT^2}{\mu^*}\ln\frac{i}{i_0}\right)\left[1-\frac{4}{C}-\frac{4kT}{C\varphi}\ln\frac{i}{i_0}\right] \tag{6}$$

$dS/d \ln i = 0$, that is Tafel slope being temperature independent we have from eq. (6)

$$C = 4+\frac{2kT}{\varphi}\ln\frac{i}{i_0} \tag{7}$$

The reciprocal of Tafel slope, is given by

$$\beta = \frac{\delta \ln i}{\delta E} = \frac{\mu^*\left(1-\frac{2\mu E^*}{C\varphi}\right)}{kT} \tag{8}$$

Various parameters of Dignam's equation can be solved using above equation

$$C = 4+\left[1+\left(\frac{1}{1+\frac{TE}{S}}\right)^2\right]^{-1} \tag{9}$$

$$\mu^* = (1+TE/S)kT\beta \tag{10}$$

$$\frac{\mu E^*}{C\varphi} = 1/2\left(1+\frac{S}{TE}\right)^{-1} \tag{11}$$

The value of μ*, C and φ were calculated from eqs. (9, 10, 11) at different current densities as a function of temperature for Nb and Ta metals in the presence of malic acid electrolyte and are tabulated in Tables 7 and 8. The values of μ*, zero field charge activation distance product, are found to increase with temperature at each set of current density. At a particular temperature, value of μ* are found to depend on current density and also on the nature of the electrolyte.

The quadratic parameter C and zero field activation energy φ are observed to be temperature independent but depend on nature of aqueous electrolyte. The quantity C and φ both change slightly with current density. The dependence of μ* and φ with the nature of electrolyte and current density were not observed by Dignam due to the non availability of steady state data for the wide range of temperature, current density and electrolyte composition.

The equation for ionic conduction can also be written as

$$I = I_0 \exp - \frac{\left[\varphi w^* E\left(1 - \ln\frac{w^* E}{2\varphi} - \frac{w^* E}{2\varphi}\right)\right]}{kT} \quad (12)$$

where w^* is the Morse function parameter and has the same dimensions as that of μ* and is given by

$$w^* = \left\{\left[1 + \frac{2}{C}\left(\frac{\mu^* C}{\varphi}\right)^2\right]^{\frac{1}{2}} - 1\right\}\frac{\varphi}{E} \quad (13)$$

The values of w^* are calculated using the values E, μ*, C and φ are found to depend on temperature, nature of electrolyte and current density. The values of the net activation energy $W(E)$ were calculated using below equation

$$W(E) = \varphi - \mu^*\left(1 - \frac{\mu^* E}{C\varphi}\right) \quad (14)$$

Table 7. Values of different parameters calculated from the Dignam's ionic conduction equations for Nb in malic acid electrolyte

Parameter	Current density	Temperature (K)			
	mA (cm^2)	293.15	303.15	313.15	323.15
μ* (eÅ)	2.5	11.00	11.05	11.13	11.19
	5.0	11.08	11.13	11.21	11.31
	10.0	11.13	11.19	11.30	11.36
	15.0	11.20	11.29	11.36	11.45
C	2.5	2.49	2.46	2.45	2.43
	5.0	2.51	2.48	2.46	2.45
	10.0	2.53	2.49	2.48	2.46
	15.0	2.54	2.51	2.49	2.48
σ (eV)	2.5	3.17	3.13	3.08	3.04
	5.0	3.19	3.15	3.11	3.08
	10.0	3.20	3.17	3.14	3.09
	15.0	3.22	3.20	3.16	3.12
W^* (eÅ)	2.5	1.22	1.15	1.15	1.00
	5.0	1.26	1.22	1.19	1.16
	10.0	1.29	1.25	1.23	1.18
	15.0	1.32	1.30	1.26	1.23
log i_0	2.5	37.72	37.08	36.42	35.78
	5.0	38.06	37.38	36.72	36.08
	10.0	38.46	37.78	36.12	36.48
	15.0	38.76	38.07	37.41	36.78

Table 8. Values of different parameters calculated from the Dignam's ionic conduction equations for tantalum in malic acid

Parameter	Current density	Temperature (K)			
	mA (cm^2)	293.15	303.15	313.15	323.15
μ* (eÅ)	2.5	6.78	7.04	7.20	7.57
	5.0	7.00	7.21	7.38	7.76
	10.0	7.12	7.34	7.53	7.92
	15.0	7.22	7.45	7.62	8.04
C	2.5	2.87	2.84	2.83	2.82
	5.0	2.91	2.88	2.87	2.86
	10.0	2.94	2.91	2.90	2.89
	15.0	2.96	2.94	2.93	2.92
σ (eV)	2.5	0.86	0.88	0.87	0.88
	5.0	0.90	0.90	0.90	0.91
	10.0	0.93	0.93	0.93	0.94
	15.0	0.95	0.95	0.94	0.95
W^* (eÅ)	2.5	1.22	1.23	1.24	1.58
	5.0	1.30	1.31	1.32	1.78
	10.0	1.34	1.37	1.38	1.84
	15.0	1.38	1.42	1.43	1.92
log i_0	2.5	17.2	17.1	16.5	16.3
	5.0	17.3	17.4	16.7	16.5
	10.0	17.7	17.5	17.2	16.8
	15.0	18.1	17.6	17.4	16.9

The values of $W(E)$ were found to be temperature, current density independent but vary with the nature of electrolyte for malic acid electrolyte. The quantity $\mu^* E/C\varphi$ measure the extent of the contribution of the quadratic term over the entire range of data and was found to be (11–13%) malic acid electrolyte.

From eqs. (4) and (14)

$$I_0 = I \exp\left(-\frac{W(E)}{[kT]}\right) \quad (14)$$

The values of log i_0 were calculated using eq. (15). The values are found to be temperature dependent and not independent as assumed by Dignam. The values of i_0 were found to change with composition of the electrolyte or current density.

The derivation of above mathematical statement assumed that the high field transfer of one kind of ionic species is responsible to control the overall rate of growth. The rate controlling step may be at the interface or inside of the film. The space charge contribution was assumed

to be zero. As there is a variation of Morse function parameters with temperature and current density, thus a single barrier theory is not strictly applicable to our data. There might be the possibility of presence of space charge in such films. It could be subsequently concluded that Dignam's methodology was not suitable for our data and there might be greater possibility of the presence of space charge in such films. From Dewald's hypothesis one can obtain

$$E(x) = E_0 + \frac{1}{\beta}\ln\left(1 + \frac{4\beta\pi q n_0 x}{\varepsilon}\right) \quad (16)$$

where $E(x)$ is the field, which is the function of thickness (x) in the oxide, E_0 is the field because to surface charge and $\beta = aq/kT$, n_0 is the number of mobile ions per cm^3 at $x = 0$ and ε is the dielectric constant of the oxide. The second part of the eq. (16) represents the contribution because of space charge and it depended on the dimensionless quantity δ, which was equivalent to $4\beta\pi q n_0 x/\varepsilon$.

Conclusions

In brief, steady state kinetics of anodic oxide film on niobium and tantalum metals has been examined at various current densities and temperatures in presence of malic acid. The constants A and B of Guntherschulze and Betz empirical equation have been determined. The value of B was found independent of temperature, which implies the non-dependence of Tafel slope on temperature. Various parameters of Dignam model i.e. zero field activation energy (f), dimensionless quantity (C), zero field activation dipole (μ^*), net activation energy $W(E)$ and More function parameter (w^*) have been evaluated and the effects of temperature, current density and nature of electrolyte on these parameters have been discussed.

References

1. A. M. Abd-Elnaiem and A. Gaber, *Int. J. Electrochem. Sci.*, 2013, **8**, 9741.
2. M. Salerno, *J. Mater. Sci. & Nanotechnol.*, 2014, **1**, 1.
3. S. S. Abdel Rehim, H. H. Hassan and M. A. Amin, *J. Appl. Electrochem.*, 2002, **32**, 1257.
4. N. I. Mukhurov, I. V. Gasenkova and I. M. Andruhovich, *J. Mater. Sci. & Nanotechnol.*, 2014, **1**, S110.
5. N. Mukherjee, M. Paulose, O. K. Varghese, G. K. Mor and C. A. Grimes, *J. Mater. Res.*, 2003, **18**, 2296.
6. M. Wang, H. Yang and Y. Liu, *Electrochim. Acta*, 2011, **56**, 7051.
7. R. L. Karlinsey, *Electrochem. Commun.*, 2005, **7**, 1190.
8. J. W. Jang, J. E. Jun and J. W. Park, *Water Sci. Technol.*, 2009, **59**, 2503.
9. H. E. Prakasam, O. K. Varghese, M. Paulose, G. K. Mor and C. A. Grimes, *Nanotechnology*, 2006, **17**, 4285.
10. J. L. Delplancke and R. Winand, *Electrochim. Acta*, 1988, **33**, 1551.
11. T. Shibata and Y. C. Zhu, *Corros. Sci.*, 1995, **37**, 133.
12. M. B. J. G. Freitas, C. Eiras and L. O. S. Buloes, *Corros. Sci.,* 2004, **46**, 1051.
13. A. Guntherschulze and H. Betz, *Z. Phys.*, 1934, **92**, 367.
14. A. T. Fromhold (Jr.) and Earl L. Cook, *Phys. Rev.*, 1967, **163**, 650.
15. M. M. Hukovic and Z. Grubac, *J. Electroanal. Chem.*, 2003, **556**, 167.
16. S. K. Poznyak, D. V. Talapin and A. I. Kulak, *J. Electroanal. Chem.*, 2005, **579**, 299.
17. C. O. A. Olsson, M. G. Verge and D. Landolt, *J. Electrochem. Soc.*, 2004, **151**, B652.
18. Pamela S. Zurer, C&EN's Washington, 2003.
19. L. Young, *Proc. Roy. Soc.*, 1966, **A258**, 496.
20. M. J. Dignam, *J. Electrochem. Soc.*, 1979, **126**, 850.
21. M. J. Dignam, *Can. J. Chem.*, 1964, **42**, 1155.